



HADRON PRODUCTION AT LARGE TRANSVERSE MOMENTUM

J. A. Appel, M. H. Bourquin, I. Gaines, D. C. Hom, L. M. Lederman,
H. P. Paar, J. -P. Repellin, D. H. Saxon, H. D. Snyder,
J. M. Weiss, and J. K. Yoh
Columbia University, New York, New York 10027

and

B. C. Brown, J. -M. Gaillard, and T. Yamanouchi
Fermi National Accelerator Laboratory, Batavia, Illinois 60510

July 1974



HADRON PRODUCTION AT LARGE TRANSVERSE MOMENTUM

J. A. Appel, M. H. Bourquin, I. Gaines, D. C. Hom, L. M. Lederman,

H. P. Paar, J.-P. Repellin^{*}, D. H. Saxon[†], H. D. Snyder,

J. M. Weiss, J. K. Yoh

Columbia University, N. Y., N. Y. 10027[‡]

and

B. C. Brown, J.-M. Gaillard^{*}, T. Yamanouchi

Fermi National Accelerator Laboratory, Batavia, Ill. 60510

ABSTRACT

We have studied production of π^0 with transverse momentum between 2.0 and 4.4 GeV/c at 65° and 93° in the center of mass system in 300 GeV proton nucleon collisions, by inserting foils of various thicknesses into a secondary beam and measuring the electron and positron spectra produced by gamma conversion. The π^0 invariant cross sections are given at 93° and 65° . We also report invariant cross sections for negatively charged hadrons as a function of transverse momentum.

The discovery of a copious yield of hadrons¹ produced at high transverse momentum provides a new tool for short range hadrodynamics. We have performed a high luminosity, large acceptance search for "direct" leptons at the Fermi National Accelerator Laboratory, observing particles produced at wide angles in 300 GeV proton-nuclear collisions. In the course of this search², we measure the spectra of electrons and positrons produced by γ conversion in thin foils. The conversion electron spectra allow us to deduce the π^0 spectra under the assumption that all of the γ 's come from π^0 decays.¹ Charged hadrons are also recorded simultaneously in this experiment.

The extracted proton beam is transported ~1.6 km to the Proton Area. The last stage of the transport system forms a parallel beam which drifts ~700 m before being brought to a $0.4 \times 3 \text{ mm}^2$ focus. The optics permit stable operation with a 40% targeting efficiency on a Be target, 0.22 mm wide and 100 mm long. The small transverse dimension of the target and the small residual matter between the target and our apparatus represent $\leq 0.9\%$ of a radiation length for conversion of γ 's in the direction of our detector.

Our apparatus is shown schematically in Fig. 1. A 9 mr x 9 mr aperture is defined by a tungsten-lined steel collimator 8.2 m long, tapered to minimize wall illumination. The production angle is measured horizontally with data taken at 50 mr and 83 mr, corresponding to 65° and 93° in the proton-nucleon center of mass system.

In order to work at high luminosity, we choose to detect particles only after magnetic deflection in the vertical plane. The "point source" target and trajectory in the vertical plane after the magnet define the momentum. The horizontal plane trajectory is used to verify the target source. The scintillation hodoscopes (210 elements) have a spatial resolution of 6 mm corresponding to a momentum resolution of 4% at 30 GeV/c. Two magnet settings cover the entire kinematic range ($P_{\perp} = 2$ to 11 GeV/c) with good efficiency and large overlap.

Particle identification is obtained using two calorimeters which follow the hodoscopes: a total absorption lead glass electromagnetic shower detector³ to identify electrons and a steel-scintillator hadron detector to separate muons from hadrons.⁴

The electromagnetic shower detector consists of two radiation lengths of lead followed by an array of 45 identical blocks of SF-5 lead glass. Scintillation counters are placed just before and immediately behind the lead. The glass blocks are arranged in 3 layers (6, 6 and 15 radiation lengths, respectively) along the particle trajectory. The hadron calorimeter contains an additional four scintillation counters for analog information and steel which, when added to the lead glass, totals 1 kg/cm^2 of iron equivalent.

An event trigger is generated by a series of scintillation counters near the hodoscopes and loose requirements in each hodoscope plane. To reduce hadrons in the electron trigger sample, a large pulse height is required in a

scintillation counter array (T2) placed after the first layer of lead glass. In addition, the total energy in the first two layers of glass is required to pass certain preset threshold levels. The lowest threshold triggers are prescaled so that a very large dynamic range in counting rate is sampled more uniformly. This trigger technique also serves to measure the trigger efficiencies for the higher threshold events.

Each block of glass and each scintillation shower counter has its signal integrated by a 1024 channel analog-to-digital converter.⁵ Calibration and stability monitoring details are described elsewhere.³ All the event information is passed to a PDP-15 computer for later analysis. The resulting electron energy resolution at 40 GeV is better than 4% FWHM with gain shifts (after corrections) of less than 1/2% due to time or entry location.

A typical plot of energy deposited in the glass (E) divided by the momentum (P) of the particle (i.e., the fraction of its energy that a particle leaves in the lead glass) for all triggers is shown in Fig. 2a. Electrons, which begin to cascade in the lead and leave all their energy in the glass, appear at $E/P = 1$, while most hadrons leave only a fraction of their energy and thus appear at $E/P < 1$. However, because of charge exchange and other processes, a significant number of hadrons (~ 1 in 2000) leave more than 90% of their energy in the glass and thus appear as a background under the electron peak at $E/P > 0.9$. Hadron rejection is improved by applying cuts on the longitudinal shower development in the array and

cuts on the signals from the scintillation counters sandwiching the two radiation lengths of lead. These cuts, about 80% efficient for electrons, result in the E/P distribution shown in Fig. 2b, where a clear electron peak is visible.

The cuts, the requirement of showering in the lead and the requirement that $0.95 < E/P < 1.05$ combine to give a hadron rejection of better than 10^4 . We also study the E/P distributions with 5 cm of lead inserted in the secondary beam producing an effectively pure hadron beam (Fig. 2c). No artificial peak appears in the cut distribution and the shape agrees with the background below the electron signal. Subtraction of this background (less than the signal even in the worst case) leaves a very clean electron peak and gives a hadron rejection of better than 10^5 .

In the π^0 experiment, we take data with foils of 2, 4 and 6% of a radiation length inserted in the secondary beam upstream of the magnets to measure the spectra of electrons and positrons produced by γ conversions. A plot of the electron yield as a function of thickness is shown in Fig. 3a. The uncorrected points are from the raw data. Corrections are then applied to take account of the energy loss due to bremsstrahlung by the electrons as they pass through the foils. The slope of the resulting line gives the number of electrons from γ conversions per 1% radiation length.

This slope is determined as a function of transverse momentum at both 50 and 83 mr to obtain the spectra shown in Fig. 3b, where the invariant cross section for electrons

from γ conversions in 1% radiation length is plotted. These data are taken on a Be target, and are normalized to a cross section per nucleon by dividing by 9, the ratio $A(\text{Be})/A(\text{H})$.⁶ Data are taken at different magnet currents which make different sections of our spectrometer sensitive to the same transverse momentum. The yields are in excellent agreement, providing a sensitive check of our understanding of the acceptance of our detector. The data are averaged over polarity since, as expected for electrons from conversions, there is no difference observed between electrons and positrons.

Figure 3c shows an invariant cross section for π^0 production at 90° which would give rise to the electron data of Fig. 3b. Systematic uncertainties in the absolute normalizations are believed to be smaller than 30%. A potentially larger error in the π^0 cross section could come from other sources of γ 's. For instance, if the η^0 is produced with the same cross section as the π^0 , its decay mode into 2 γ 's would mean we have overestimated the π^0 cross section by about 35%.

We have at the same time measured charged hadron spectra with a trigger that complemented the electron trigger and also used the information from the hadron calorimeter to reject muons and backgrounds.

The resulting P_\perp distribution for negative hadrons (expected to be about 80% π^-)⁷ is given in Fig. 3c. Also shown is a fit to the π^0 spectrum of the CERN-Columbia-Rockefeller Collaboration (CCR)¹ modified to fit smoothly at moderate P_\perp

$$E \frac{d^3\sigma}{dp^3} = \frac{15 \text{ mb}}{(p_{\perp}^2 + 1)^4} e^{-13 x_{\perp}}, \quad x_{\perp} = \frac{2p_{\perp}}{\sqrt{s}} \quad (1)$$

and the average of the charged pion spectra measured at Fermi-Lab by the Chicago-Princeton Group reduced from Be to p-nucleon using the same factor of A.⁶

The π^0 data at 90° are in excellent agreement with the modified CCR fit. Furthermore, the invariant cross sections at 65° and 93° are very similar indicating that any angle dependence beyond that given in Eq. 1 is not large.

Finally, charged hadrons spectra have a slope indistinguishable from that of the π^0 . These data also agree very well with the FermiLab work of Cronin et al. for $x_{\perp} < 0.5$ ⁷

It is a pleasure to thank the staff of the Fermi National Accelerator Laboratory and especially of the Proton Section for their efforts. We are also deeply indebted to Messrs. T. E. Nureczyk, F. H. Pearsall, and S. J. Upton and the staff of Nevis Laboratories for their help in the design and implementation of the apparatus.

FOOTNOTES AND REFERENCES

*Permanent address: Laboratoire de l'Accélérateur
Linéaire, Orsay, France

†Present address: Rutherford High Energy Laboratory,
Chilton, Didcot, Berkshire, England.

‡Research supported by the National Science Foundation.

¹F. W. Büsser et al., Phys. Letters 46B, 471 (1973). See
also B. Alper et al., Phys. Letters 44B, 521 (1973).

M. Banner et al., Phys. Letters 44B, 537 (1973).

²J. A. Appel et al., Observation of Direct Production of
Leptons in p-Be Collisions at 300 GeV, following Letter.

³The calibration, stability, resolution, and hadron rejection
of the lead glass is discussed more fully in "Performance
of a Lead Glass Electromagnetic Shower Detector at FermiLab,"
to be published.

⁴M. H. Bourquin and D. H. Saxon, Nucl. Inst. & Meth. 108, 461
(1973).

⁵F. W. Sippach, to be published.

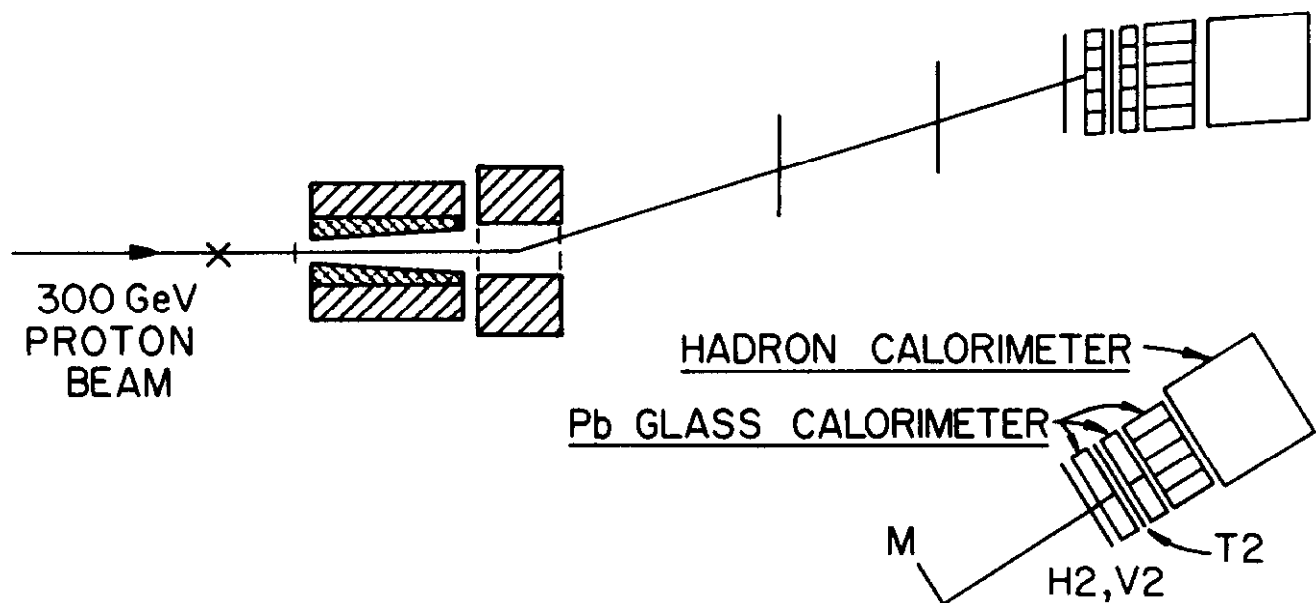
⁶J. W. Cronin et al., Preprint. "Atomic Number Dependence
of Hadronic Production at Large Transverse Momentum," Session
A3, HEPC, London (1974).

⁷J. W. Cronin et al., Phys. Rev. Letters 31, 1426 (1973).

FIGURE CAPTIONS

- Fig. 1 Experimental Apparatus for Electron and Gamma Study.
- Fig. 2a E/P distribution with no cuts.
- Fig. 2b E/P with shower cuts.
- Fig. 2c E/P with shower cuts and with 5 cm. Pb which removes all electrons.
- Fig. 3a Yield of electrons vs. foil thickness.
- Fig. 3b Invariant cross section for conversion electrons.
The errors shown are statistical only.
- Fig. 3c Invariant cross sections near 90° :
- a) π^0 's, this experiment,
 - b) CCR modified fit,
 - c) h^- this experiment,
 - d) $(\pi^+ + \pi^-)/2$ Chicago-Princeton

SIDE VIEW



TOP VIEW

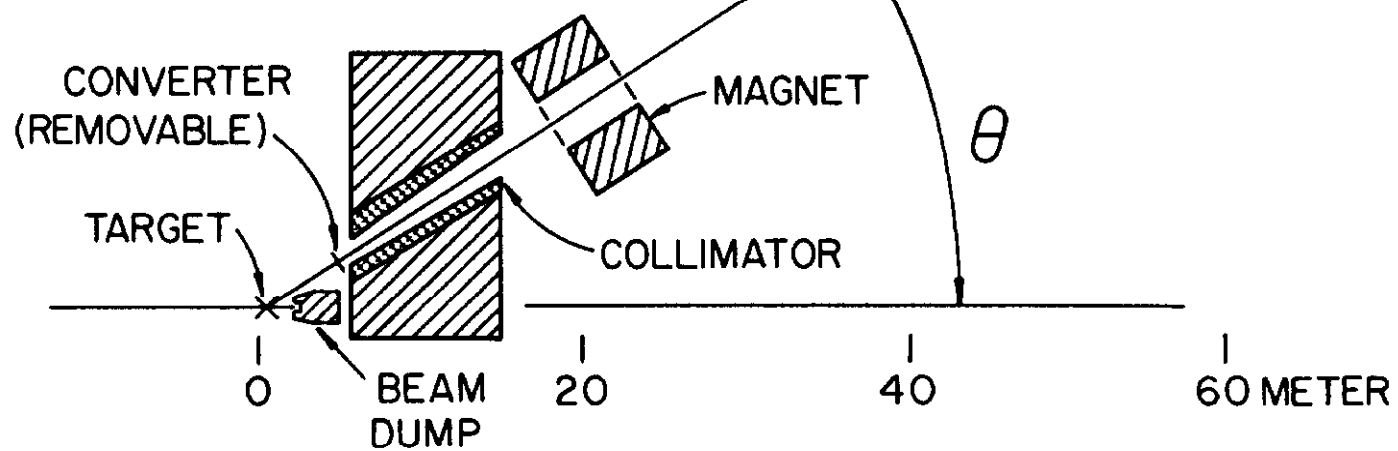


Fig. 1

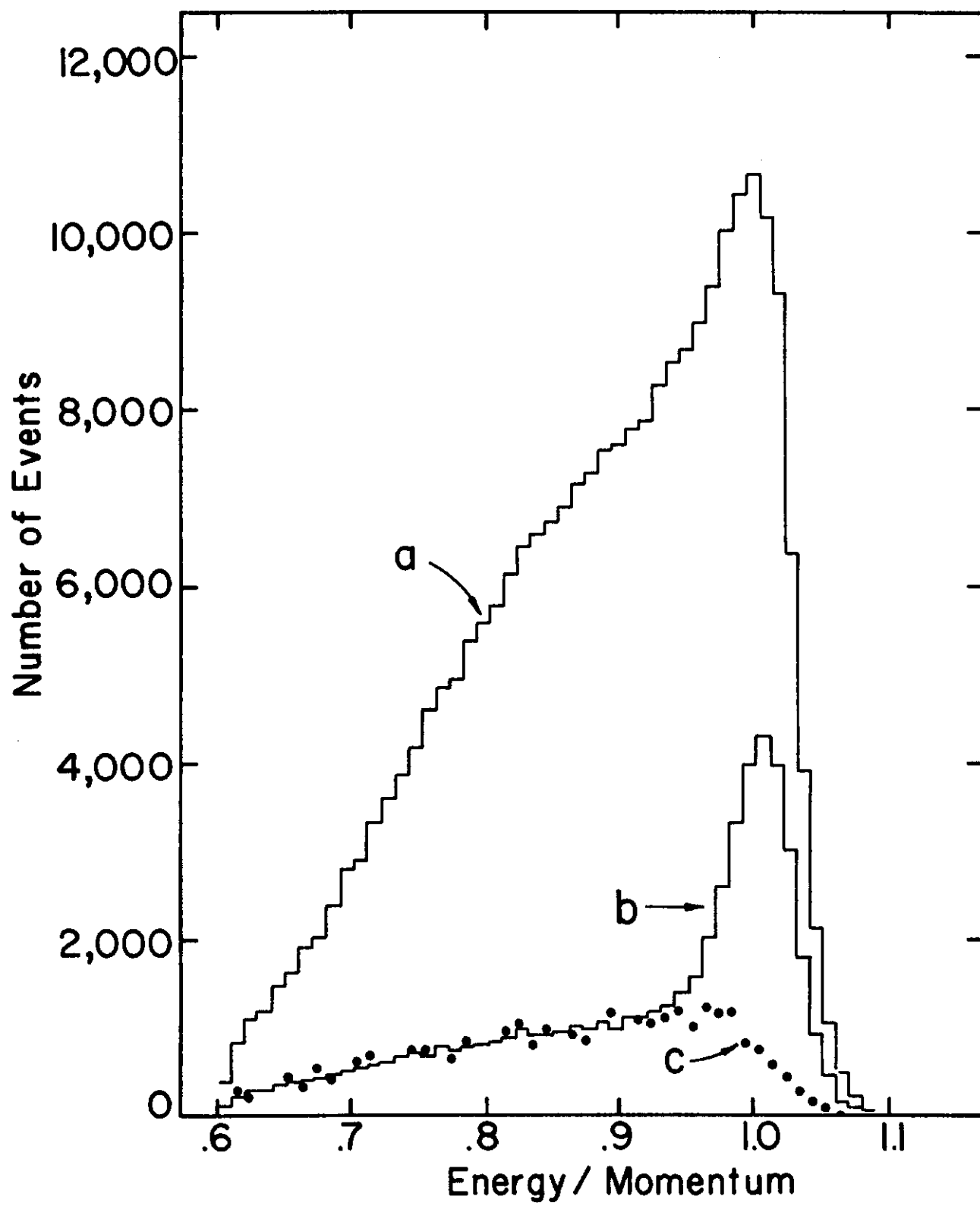


Fig. 2

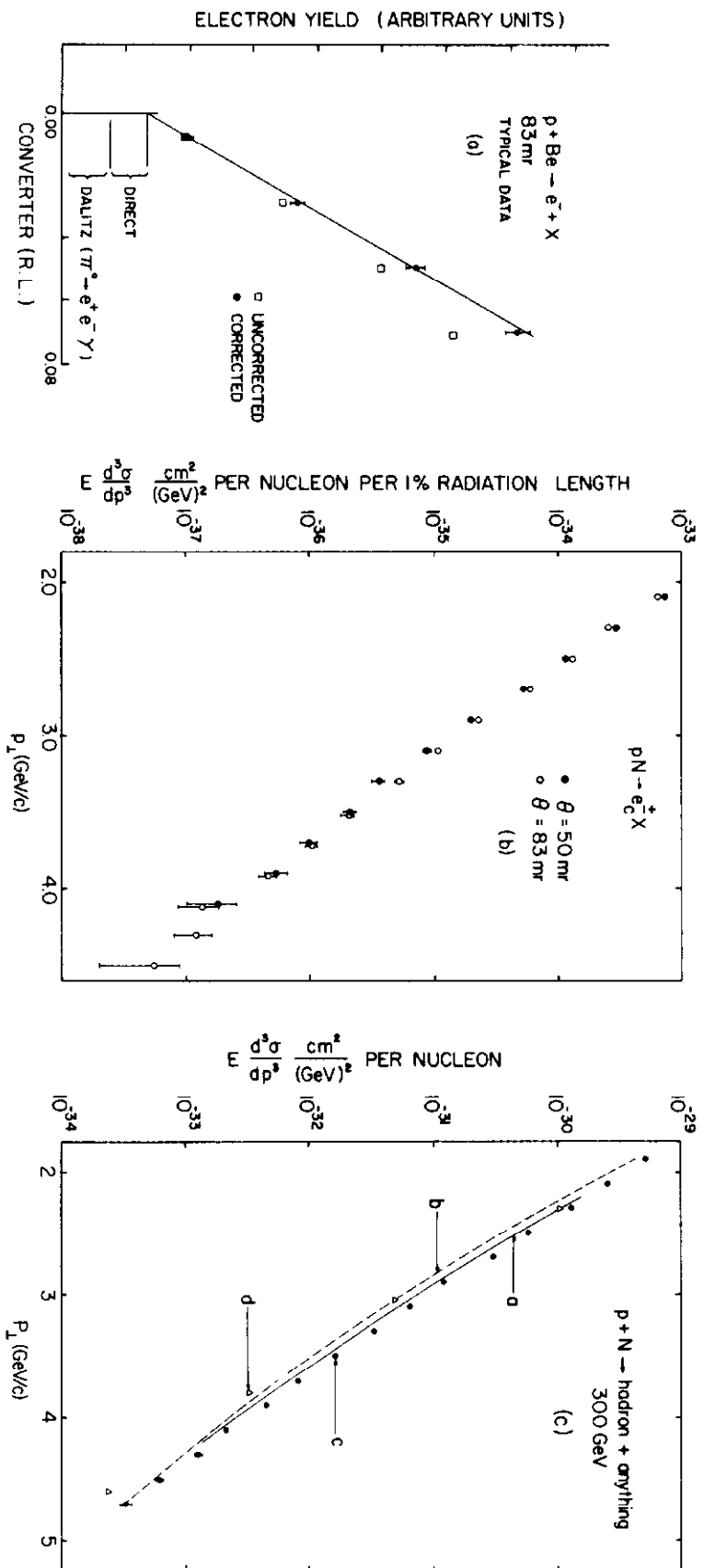


Fig. 3